Faculty of Pharmaceutical Sciences, Khon Kaen University, Khon Kaen, Thailand

Characterization of microcrystalline cellulose loaded diclofenac calcium alginate gel beads *in vitro*

T. PONGJANYAKUL

Received November 11, 2006, accepted December 20, 2006

Thaned Pongjanyakul, PhD, Faculty of Pharmaceutical Sciences, Khon Kaen University, Khon Kaen 40002, Thailand
thaned@kku.ac.th

Pharmazie 62: 493–498 (2007) *doi: 10.1691/ph.2007.7.6260*

Diclofenac calcium alginate (DCA) beads containing microcrystalline cellulose (MCC) were prepared using ionotropic gelation method. The effect of MCC amounts on physicochemical characteristics of the DCA beads was examined. The particle size and entrapment efficiency of diclofenac sodium (DS) of the DCA beads increased with increasing amount of MCC. MCC could be involved in the calcium alginate formation to create a complex matrix in the DCA beads, which was revealed using FTIR spectroscopy. The MCC-DCA beads provided greater water uptake in distilled water, but retarded swelling rate in pH 6.8 phosphate buffer. A longer lag time and a similar drug release rate of the MCC-DCA beads in pH 6.8 phosphate buffer were found. The MCC-DCA beads also gave higher drug release rates in distilled water when compared with the DCA beads. However, the increase of MCC content over 0.5% in the DCA beads did not affect the drug release in distilled water. In conclusion, MCC could improve drug entrapment efficiency and modify drug release from the DCA beads.

1. Introduction

Sodium alginate (SA) has been widely used as food and pharmaceutical additive, such as a tablet disintegrant, a thickening and a suspending agent. It contains two uronic acids, α-L-guluronic and β-D-mannuronic acids, and is composed of homopolymeric blocks and blocks with an alternating sequence (Draget 2000). Gelation occurs by cross-linking of the uronic acids with divalent cations, such as Ca^{2+}. The primary mechanism of this gelation involves extended chain sequences which adapt a regular twofold conformation and dimerize with specific chelation of Ca^{2+}, the so-called 'egg-box' structure (Grant et al. 1973). Each Ca^{2+} ion takes part in nine co-ordination links with an oxygen atom, resulting in three-dimensional network of calcium alginate. This phenomenon has been applied for preparing an alginate bead employed as a drug delivery system by dropping the drug-containing SA dispersion into a calcium chloride bath (Østberg et al. 1994; Sugawara et al. 1994). The calcium alginate bead could protect an acid-sensitive drug from gastric juice, and the drug was consequently released from the bead in the intestine (Hwang et al. 1995; Fernández-Hervás et al. 1998). Thus, drug-loaded alginate beads are suitable for nonsteroidal anti-inflammatory drugs, which cause gastric irritation. Moreover, the alginate beads also exhibit a potential for a pulsatile release system of macromolecular drugs (Kikuchi et al. 1997).

Incorporation of some substances could modulate physical properties of calcium-alginate beads. Water-soluble polymers, such as chondroitin sulfate (Murata et al. 1996), konjac glucomannan (Wang and He 2002), gelatin (Almeida and Almeida 2004), sodium starch glycolate (Puttipipatkhachorn et al. 2005), and xanthan gum (Pongjanyakul and Puttipipatkhachorn 2007) have been used to reinforce calcium alginate beads because of complex formation of alginate with such water-soluble polymers. Chitin, a water-insoluble polymer, was added into the beads so as to retard drug release in pH 6.8 dissolution medium. This was owing to the formation of a complex between the carboxyl groups of alginate and the amino groups of chitin (Murata et al. 2002). Furthermore, insoluble substances, such as wax particles (Kim et al. 2005; Pongjanyakul et al. 2006) and magnesium aluminum silicate (Puttipipatkhachorn et al. 2005), could improve drug entrapment efficiency and retard drug release from the beads due to an increase in hydrophobic property and an interaction of silanol groups of magnesium aluminum silicate with carboxyl groups of alginate, respectively.

In the present study, microcrystalline cellulose (MCC) was selected to be incorporated into diclofenac calcium alginate (DCA) beads. MCC is purified, partially depolymerized cellulose. It is widely used in pharmaceuticals primarily as a diluent in oral tablet and capsule formulations (Wade and Weller 1994) and also applied as a main component to prepare granules (Johansson and Alderborn 2001) and pellets (Johansson et al. 1995; Johansson and Alderborn 1996). Hwang et al. (1995) reported that MCC loaded in ibuprofen calcium alginate beads could increase drug release rate in simulated intestinal fluid at pH 6.8. However, other characteristics of the beads having MCC have not yet been examined. Therefore, the DCA beads containing different amounts of MCC were prepared with ionotropic gelation method and calcium ions were used as

cross-linking agents. Physicochemical properties of the MCC-DCA beads, such as entrapment efficiency of diclofenac sodium (DS), thermal behavior, water uptake, swelling, and drug release in various dissolution media were investigated. Interaction of MCC and SA in the DCA beads was examined using FTIR spectroscopy as well.

2. Investigations, results and discussion

2.1. DSC and FTIR studies

DSC thermogram of DS showed an endothermic peak at 55 °C (Fig. 1a). This was due to the evaporation of the water of crystallization (Palomo et al. 1999). The sharp exothermic peak of DS at 280 °C and a small endothermic peak at 284 °C indicated an oxidation reaction between DS and oxygen in air environment and a melting of the compound, respectively (Tudja et al. 2001). MCC showed endothermic and exothermic decomposition peaks around 320 and 350 °C, respectively (Fig. 1b). The DCA beads presented a broad endothermic peak at 65 °C because of residual water evaporation from the beads and no peaks of DS were observed (Fig. 1c), indicating DS was molecularly dispersed in the calcium alginate matrix. Incorporating MCC into the DCA beads presented no different thermogram (Fig. 1d–f). This indicated that MCC did not affect the thermal property of the DCA beads. However, the MCC-DCA beads did not present the endothermic and exothermic peaks of MCC, although 3% MCC was added in the bead preparation. This suggested that MCC may interact with SA in cross-linking process.

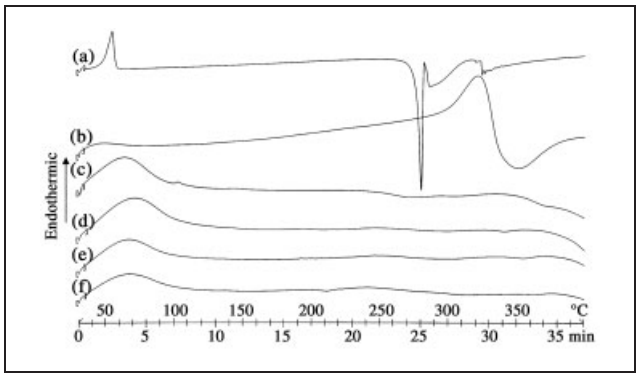

Fig. 1: DSC thermograms of DS (a), MCC (b), DCA beads prepared using 0% (c), 0.5% (d), 1% (e) and 3% MCC (f)

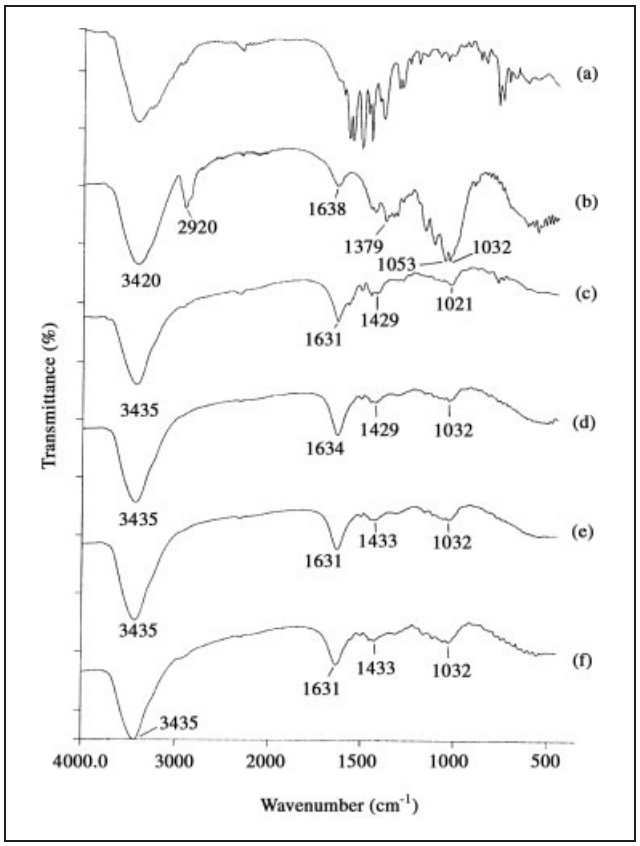

Fig. 2: FTIR spectra of DS (a), MCC (b), DCA beads prepared using 0% (c), 0.5% (d), 1% (e) and 3% MCC (f)

FTIR spectra of SA showed the peaks around 3435, 1615, 1418, and 1031 cm^{-1}, indicating the stretching of O−H, COO^- (asymmetric), COO^- (symmetric), and C−O−C, respectively. The cross-linking process with calcium ion caused an obvious shift to higher wavenumbers and a decrease in intensity of COO^- stretching peaks, and a decrease in intensity of 1031 cm^{-1} peak of SA, which were previously reported (Puttipipatkhachorn et al. 2005; Pongjanyakul and Puttipipatkhachorn 2007). This indicated an ionic bonding between calcium ion and carboxyl groups of SA and a partial covalent bonding between calcium and oxygen atom of ether groups, respectively. The spectra of the DCA beads presented the peaks of DS at around 1386–1575 cm^{-1} (Fig. 2c). Incorporation of MCC into the DCA beads obviously provided a shift to higher wavenumber of C−O−C stretching peak at 1021 cm^{-1} and no change of COO^- stretching peaks at 1631 and 1429 cm^{-1} was found (Fig. 2d–f). Moreover, it can be seen that FTIR spectra of the DCA beads with MCC did no present the peaks of MCC, although 3% MCC was used. This suggested that MCC could be involved in the calcium alginate formation to create a complex matrix in the DCA beads.

2.2. Physical properties of the MCC-DCA beads

MCC used in this study was composed of large and irregular particles, among which were numerous small more regularly shaped particles. The DCA and the MCC-DCA beads were quite spherical (Fig. 3a and 3b). The surface morphology of the MCC-DCA beads did not show MCC particles. This indicated that MCC particles were embedded in the bead matrix. It can be seen that the higher the MCC content, the greater the particle size of the DCA beads (Table 1). The DS entrapment efficiency of the MCC-DCA beads increased significantly ($P < 0.05$) with increasing amount of MCC, suggesting that MCC caused an increasing barrier preventing water leakage from the beads during the preparation period (Dashevsky 1998). Furthermore, the greater particle size of the MCC-DCA beads had a longer pathlength for drug diffusion from the beads. These led to reduced drug loss from the beads. To

Table 1: Particle size and drug entrapment efficiency of MCC-DCA beads

Component	Particle size[a] (mm)	DS entrapment efficiency[b] (%)
1.5% w/v SA	1.37 ± 0.11	39.8 ± 2.7
+0.5% w/v MCC	1.43 ± 0.14	43.3 ± 1.0
+1.0% w/v MCC	1.57 ± 0.19	50.0 ± 1.0
+3.0% w/v MCC	1.85 ± 0.21	64.4 ± 1.7

[a] Data are mean ± S.D., n = 250
[b] Data are mean ± S.D., n = 3

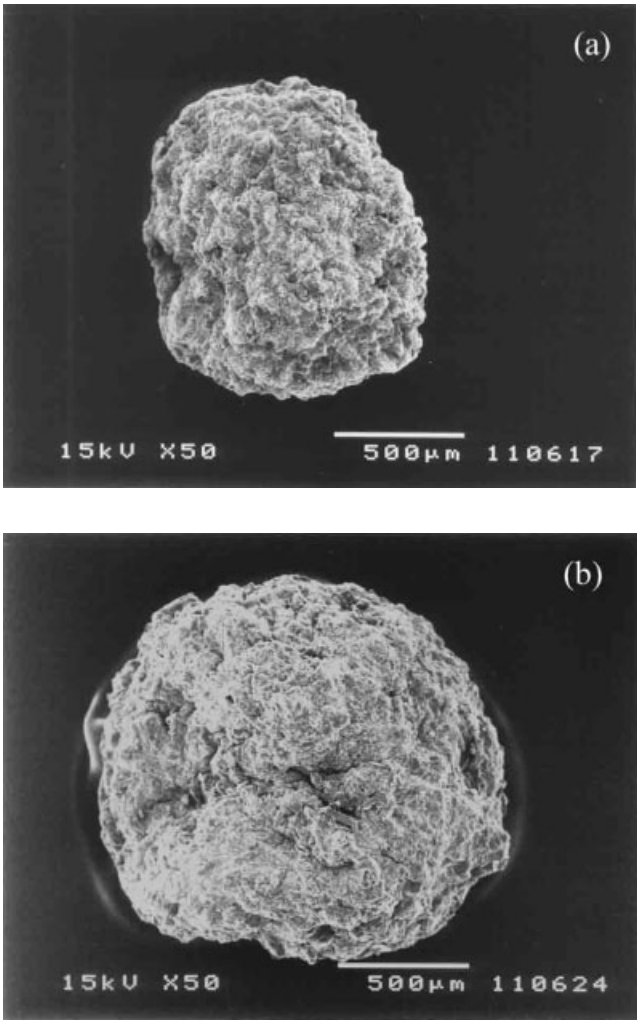

Fig. 3: SEM picture of DCA bead (a) and 3% MCC-DCA bead (b)

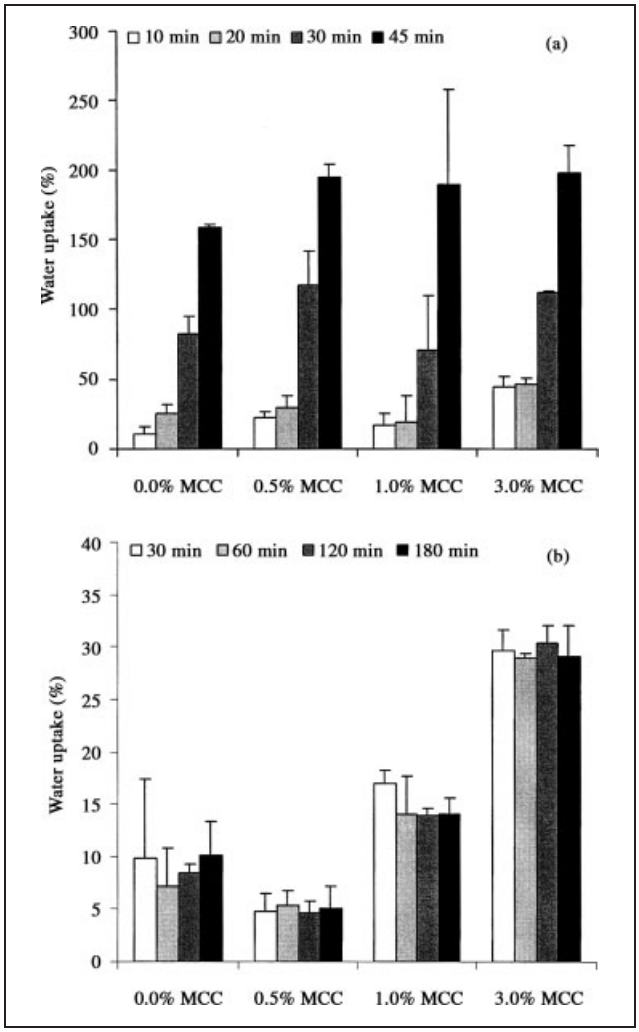

Fig. 4: Water uptake of DCA beads having different amounts of MCC in pH 6.8 phosphate buffer (a) and distilled water (b). Each value is the mean ± S.D., n = 3

compare with the effect of magnesium aluminum silicate (MAS) and glyceryl palmitostearate (GPS) on DS entrapment efficiency of the DCA beads, which were previously reported by Puttipipatkhachorn et al. (2005) and Pongjanyakul et al. (2006), respectively. The DS entrapment efficiency of the MCC-DCA beads was remarkably higher than that of the MAS-DCA beads, but obviously lower than that of the GPS-DCA beads. This can be explained by the properties of additive added into the DCA beads. MAS is composed of thousands of submicroscopic platelets and this structure could be separated when MAS was dispersed in water. The size of MAS platelets is very small when compared with the particle size of MCC. This indicated that MCC and MAS could form the different structure matrix of the wet DCA beads, which MCC may create a denser matrix than MAS in the wet DCA beads during preparation. In contrast, GPS is a waxy substance that could enhance a hydrophobic property to the wet DCA beads, resulting in a retardation of drug leakage from the wet DCA beads.

2.3. Water uptake and swelling of the MCC-DCA beads

The water uptake of the MCC-DCA beads in pH 6.8 phosphate buffer is shown in Fig. 4a. The % water uptake of the DCA beads in pH 6.8 phosphate buffer increased with increasing time of testing. The 3% MCC-DCA beads provided obviously higher %water uptake than the DCA beads. The %water uptake in distilled water was significantly lower ($P < 0.05$) than that in pH 6.8 phosphate buffer (Fig. 4b). The equilibrium time of water uptake in distilled water of the DCA beads was about 30 min. Incorporation of 0.5% and 1% MCC into the DCA beads did not obviously affect the water uptake, but the 3% MCC-DCA beads gave a statistically higher ($P < 0.05$) water uptake in distilled water when compared with the DCA beads.

The swelling profiles of the MCC-DCA beads in pH 6.8 phosphate buffer and distilled water are shown in Fig. 5. In pH 6.8 phosphate buffer, the swelling equilibrium time of the DCA beads was approximately 120 min (Fig. 5a). The %swelling of the DCA beads decreased with increasing amount of MCC. The swelling rate of the DCA beads in pH 6.8 phosphate buffer could be obtained from the slope of the relationship between the % swelling and the square root of time (Lee and Peppas 1987; Puttipipatkhachorn et al. 2005; Pongjanyakul and Puttipipatkhachorn 2007). This relationship provided a good linearity with R^2 more than 0.98 when analyzed by linear regression analysis (Table 2). Addition of MCC into the DCA beads caused a significant decrease ($P < 0.05$) in swelling rate of the MCC-DCA beads. In distilled water, the swelling rate of the DCA beads cannot be estimated because of lower swelling of the DCA beads in this medium. How-

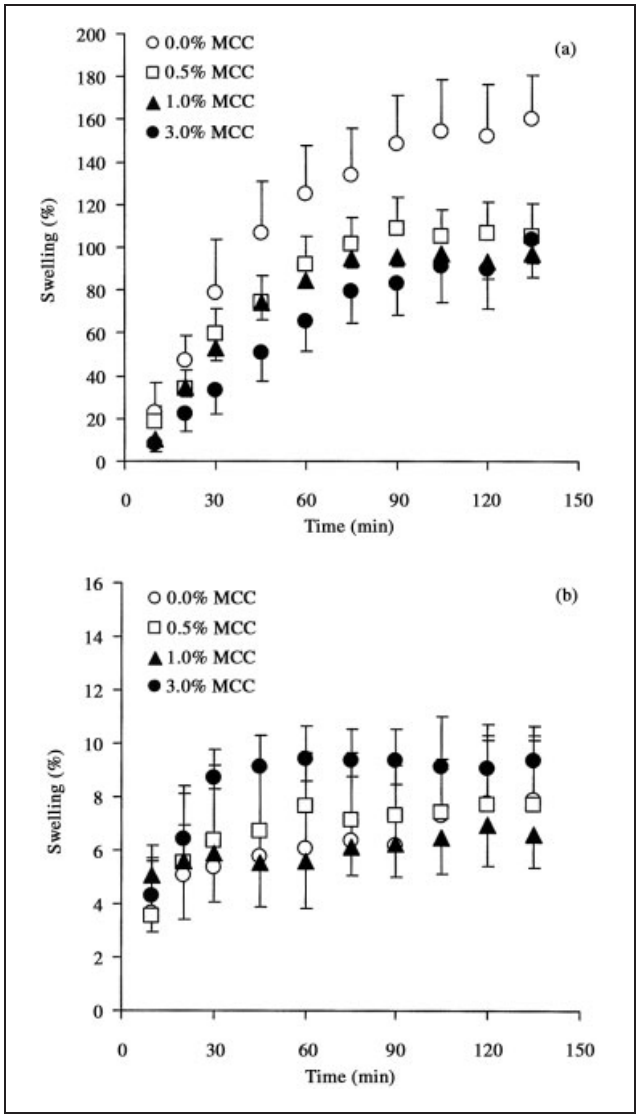

Fig. 5: Swelling profiles of DCA beads having different amounts of MCC in pH 6.8 phosphate buffer (a) and distilled water (b). Each point is the mean ± S.D., n = 5

ever, the % swelling of the DCA beads tended to increase when increasing the MCC content to 3% (Fig. 5b).

Water uptake and swelling of the DCA beads in pH 6.8 phosphate buffer were higher than those in distilled water because calcium ions cross-linked with alginate were rapidly exchanged with sodium ions in phosphate buffer (Østberg et al. 1994). The partial formation of SA induced water uptake into the beads. Moreover, calcium alginate gels could be solubilized by the addition of phosphate ions, which acted as calcium ions complexing agent at a pH above 5.5 (Remuñán-López and Bodmeier 1997). This caused an unclear water uptake effect of MCC in the DCA beads when using pH 6.8 phosphate buffer. However, incorporating MCC decreased the % swelling and swelling rate of the DCA beads because of no swelling capacity of MCC (Chebli and Cartilier 1998). MCC embedded in the DCA beads could stabilize the dimension of the beads at the initial period of swelling. This can be attributed to the interfacial interaction between MCC and SA in the beads. In distilled water, MCC could promote the water uptake of the DCA beads since calcium-alginate beads existed as a stable polymer matrix. Moreover, the increase in water uptake of the DCA beads depended on the amount of MCC added, which could be obviously observed in the 3% MCC-DCA beads. However, a small effect of MCC on swelling of the DCA beads in this medium was found due to the lake of swelling capacity of MCC.

2.4. In vitro release from the MCC-DCA beads

The release profiles of DS from the MCC-DCA beads in pH 6.8 phosphate buffer and distilled water are shown in Fig. 6. The release profile of DS in pH 6.8 phosphate buffer showed a sigmoidal profile with a complete release (Fig. 6a) and the disintegration of the swollen beads occurred around 75–90 min of the test. A lag time and a release rate of DS were obtained from fitting the data into zero-order model, which a good linearity with R^2 higher than 0.98 was found. This indicated a swelling controlled mechanism. The lag times of the 0.5% and 1% MCC-DCA beads were not different, but the 3% MCC-DCA beads gave a statistically longer ($P < 0.05$) lag time when compared with the DCA beads (Table 2). However, incorporating MCC did not affect the DS release rate of the DCA beads (Table 2). In distilled water, incomplete release of DS for 8 h was found (Fig. 6b). The release of DS in this medium did not show the lag time and can be described using Higuchi's model. The DCA beads gave lower release rate than the MCC-DCA beads, whereas the same release rate of the 0.5–3% MCC-DCA beads was observed. SEM photographs showed that the erosion of the surface of the DCA beads and the 3% MCC-DCA beads after release testing in distilled water was similar and no pore formation was found in the 3% MCC-DCA beads (data not shown). The erosion of the DCA beads could be observed because a residual alginate could release from the beads (Murata et al. 1993), which occurred from a small amount of calcium ion released in distilled water (Østberg et al. 1994).

The release of DS from the DCA beads in pH 6.8 phosphate buffer was depressed by the formation of the gel layer at the initial stage but gradually enhanced by the increasing water content and the erosion of the swollen gel phase at the later stage (Sugawara et al. 1994). This

Table 2: Swelling and drug release rate of MCC-DCA beads

Component	pH 6.8 phosphate buffer			Distilled water
	Swelling rate[a] (% $min^{-1/2}$)	Release rate[b] (% min^{-1})	Lag time[b] (min)	Release rate[b] (% $min^{-1/2}$)
1.5% w/v SA	21.7 ± 3.6 ($R^2 = 0.983$)	1.28 ± 0.05 ($R^2 = 0.988$)	19.4 ± 0.7	3.12 ± 0.09 ($R^2 = 0.995$)
+0.5% w/v MCC	16.2 ± 2.0 ($R^2 = 0.985$)	1.27 ± 0.04 ($R^2 = 0.994$)	17.7 ± 0.5	4.61 ± 0.07 ($R^2 = 0.990$)
+1.0% w/v MCC	16.9 ± 2.8 ($R^2 = 0.987$)	1.24 ± 0.06 ($R^2 = 0.992$)	20.1 ± 0.5	4.55 ± 0.01 ($R^2 = 0.995$)
+3.0% w/v MCC	12.8 ± 2.1 ($R^2 = 0.986$)	1.22 ± 0.01 ($R^2 = 0.998$)	25.2 ± 0.5	4.41 ± 0.02 ($R^2 = 0.993$)

[a] Data are mean ± S.D., n = 5
[b] Data are mean ± S.D., n = 3

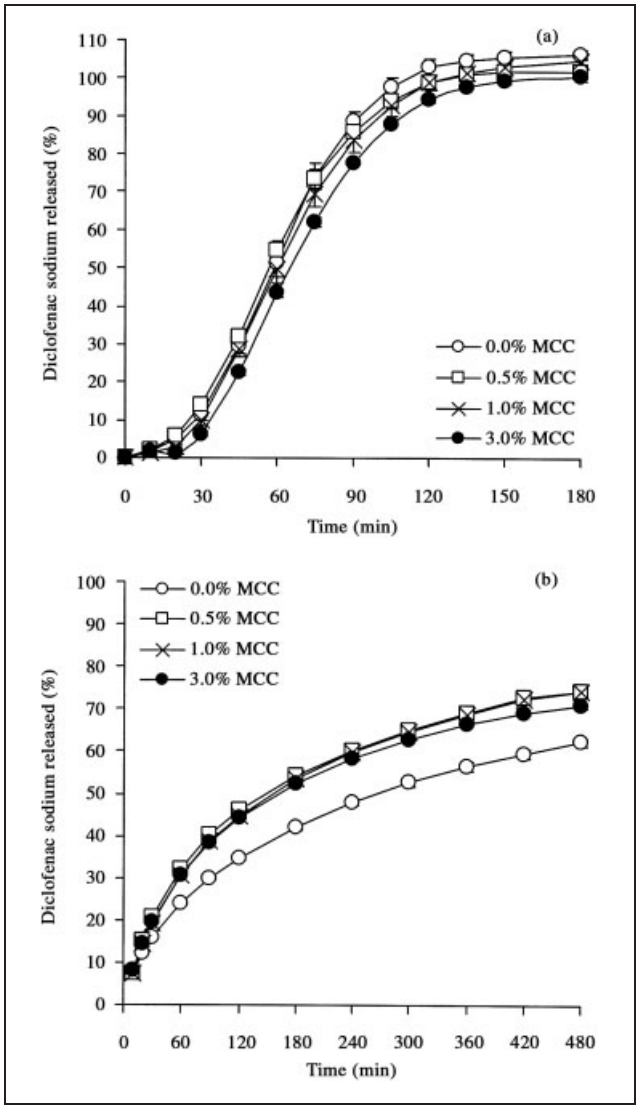

Fig. 6: Drug release profiles of DCA beads having different amounts of MCC in pH 6.8 phosphate buffer (a) and distilled water (b). Each point is the mean ± S.D., n = 3

can be described by the ion exchange between calcium ion in the beads and sodium ion in the medium. Calcium ions interacted with carboxylic groups in alginate, but not participating in the egg-box formation, are preferentially released through ion exchange with sodium ion in the medium. Almost negligible alginate disintegration at this stage was probably due to the relatively stable association of calcium ions with polyguluronate sequences, which served as stable cross-linking points within the gels. Alginate disintegration occurred when the calcium ions in the egg-box structure started to release for exchange with sodium ions (Kikuchi et al. 1997). Furthermore, the lag time of release profile occurred because the solubility of DS was decreased in the presence of sodium ions. This can be attributed to the common ion effect (Sheu et al. 1992). Incorporation of MCC into the DCA beads gave longer lag time of DS release because MCC retarded the swelling rate of the DCA beads that caused a slower DS release in the initial stage. However, MCC did not affect tortuosity of swollen beads. This led to the same DS release rate.

The release of DS from the DCA beads in distilled water was slower than that in pH 6.8 phosphate buffer because the DCA beads were stable with the small amount of calcium released (Østberg et al. 1994). Thus, the release mechanism of DS from the beads was matrix diffusion-controlled. MCC could accelerate the DS release from the beads. This was because of increased hydrophilic properties of the beads. However, all MCC-DCA beads gave the same release rate, although 3% MCC-DCA beads had the highest water uptake. This suggested that an increase in water uptake of the 3% MCC-DCA beads may cause a decrease in the tortuosity of the matrix structure when compared with the DCA beads with lower content of MCC. Moreover, MCC cannot create pore channels in the DCA beads. By these reason, the higher MCC content in the DCA beads did not accelerate the drug release.

The effect of MCC on the DS release of the DCA beads was in contrast to that of MAS (Puttipipatkhachorn et al. 2005). The 3% MAS-DCA beads could retard drug release in pH 6.8 phosphate buffer, although swelling and water uptake of these beads were similar to the 3% MCC-DCA beads. This suggested that the 3% MAS-DCA beads could provide higher tortuosity than the 3% MCC-DCA beads because the interaction of SA with MAS was stronger than that with MCC in the reswollen beads. This reason can also be used to explain drug release in distilled water where the MAS-DCA beads gave slower drug release than the DCA beads and the MCC-DCA beads.

In conclusion, incorporation of MCC into the DCA beads could modify the physicochemical properties of the beads because of the interaction of MCC with SA in the matrix structure. The MCC-DCA beads provided higher drug entrapment efficiency and greater water uptake in distilled water, but retarding swelling rate in pH 6.8 phosphate buffer. A longer lag time and a similar drug release rate of the MCC-DCA beads in pH 6.8 phosphate buffer were found. In distilled water, the MCC-DCA beads gave higher drug release rates than the DCA beads, but increasing MCC content above 0.5% did not affect drug release.

3. Experimental

3.1. Materials

Diclofenac sodium (DS) was a gift from Biogena Ltd (Limassol, Cyprus). Sodium alginate NF17 and microcrystalline cellulose (Avicel®PH102, MCC) were purchased from Srichand United Dispensary Co., Ltd (Bangkok, Thailand) and Asahi Chemical Industry Co., Ltd (Tokyo, Japan). All other reagents used in this study were of analytical grade and used as received.

3.2. Bead preparation

SA (1.5% w/v) was dispersed in distilled water with agitation, and then DS (1% w/v) was added and completely dissolved with a homogenizer for 5 min. DS-SA dispersion (80 ml) was dropped through a 1.2 mm inner diameter needle, from a hypodermic syringe into 0.45 M calcium chloride solution (200 ml). The DCA beads were cured in this solution for 1 h, then filtered, and rinsed several times with distilled water. The beads were dried at room temperature for 48 h, followed at 45 °C for 12–16 h. To prepare the MCC-DCA beads, MCC (0.5, 1 and 3% w/v) was incorporated into the DS-SA dispersion using a homogenizer for 5 min and then the preparation was proceeded as described above.

3.3. Fourier transformed infrared (FTIR) spectroscopy

FTIR spectra of DS, MCC and DCA beads were recorded with a FTIR spectrophotometer (Spectrum One, Perkin Elmer, Norwalk, CT) using KBr disc method. Each sample was gently triturated with KBr powder in a weight ratio of 1 : 100 and then pressed in a hydrostatic press at a pressure of 10 tons for 5 min. The disc was placed in the sample holder and scanned from 4000 to 450 cm^{-1} at a resolution of 4 cm^{-1}.

3.4. Differential scanning calorimetry (DSC)

DSC thermograms of DS, MCC and DCA bead were recorded using a differential scanning calorimeter (DSC822, Mettler Toledo, Switzerland). Each sample (2.0–2.5 mg) was accurately weighed into a 40-µl aluminum pan without an aluminum cover. The measurement was performed over 30–400 °C at a heating rate of 10 °C/min.

3.5. Particle size determination

Particle size of the DCA beads was determined using an optical microscope (Nikon, Japan). Two hundred fifty beads were randomized and their Feret's diameters were measured and the mean diameters were calculated.

3.6. Drug entrapment efficiency determination

Weighed DCA beads were immersed and dispersed in 100 ml of 0.067 M phosphate buffer at pH 6.8 for 12 h. Then, the solution was filtered, and the DS content was assayed by an UV-spectrophotometer (Shimadzu UV1201, Kyoto, Japan) at 260 nm. The ratio of the actual to the theoretical drug contents in the DCA beads was termed as entrapment efficiency (Wang and He 2002).

3.7. Scanning electron microscopic studies

Surface morphology of DCA beads was characterized before and after release testing in distilled water. Particle shape of MCC was investigated as well. Samples of the dried beads were mounted onto stubs, sputter coated with a gold in a vacuum evaporator, and photographed using a scanning electron microscope (Jeol Model JSM-5800LV, Tokyo, Japan).

3.8. Water uptake determination

Weighed DCA beads were placed in a small basket, soaked in 0.067 M phosphate buffer at pH 6.8 or distilled water and shaken occasionally at room temperature ($26 \pm 1\,^{\circ}C$). After a predetermined time interval, each basket was withdrawn, blotted to remove excess water and immediately weighed on an analytical balance (Remuñán-López and Bodmeier 1997). The water uptake can be calculated from the following equation:

$$\text{Water uptake}\,(\%) = \left(\frac{W_t - W_0}{W_0}\right) \times 100 \qquad (1)$$

where W_t and W_0 are the wet and initial mass of beads, respectively. Water uptake study of DCA beads in pH 6.8 phosphate buffer was performed for 45 min because the swollen beads were broken and could not be blotted to remove excess water at the longer time.

3.9. Swelling studies

The diameter of DCA beads were measured using a digital caliper (Mitutoyo Model 500-136, Kawasaki, Japan) and then placed in petri disk containing 20 ml of 0.067 M phosphate buffer at pH 6.8 or distilled water at room temperature ($26 \pm 1\,^{\circ}C$). At predefined time intervals, the diameter of each bead was determined at two different positions, and swelling (%) of the beads was calculated according to Eq. (2) (Talukdar and Kinget 1995).

$$\text{Swelling}\,(\%) = \left(\frac{D_t - D_0}{D_0}\right) \times 100 \qquad (2)$$

where D_0 and D_t are the initial diameter of the beads and the diameter of the beads at a given time, respectively.

3.10. In vitro drug release studies

A USP dissolution apparatus I (Hanson Research, Northridge, CA) was used to characterize the release of DS from the DCA beads. The baskets were rotated at 50 rev/min at $37.0 \pm 0.5\,^{\circ}C$. The dissolution media used were 0.067 M phosphate buffer at pH 6.8 or distilled water. The amount of the DCA beads added to 750 ml dissolution medium was equivalent to DS 25 mg. Samples (7 ml) were collected and replaced with a fresh medium at various time intervals. The amount of drug released was analyzed spectrophotometrically at 260 nm (Shimadzu UV1201, Japan).

The DS release kinetics from the DCA beads in various dissolution media were investigated by fitting the DS release data into zero order and Higuchi's model, which can be expressed by Eq. (3) as followed:

$$Q = kt^n \qquad (3)$$

where Q is the percentage of drug released at a given time (t), k is the release rate and n is the diffusion exponent. The n value could be defined as 0.5 and 1, which indicated the Higuchi's and zero order equation, respectively (Costa and Lobo 2001). The release rate was estimated by fitting the experimental drug release data into both models and analyzed by linear regression analysis.

3.11. Statistical analysis

One-way analysis of variance (ANOVA) with the least significant difference (LSD) test for multiple comparisons (SPSS program for MS Windows, release 10.0) was performed to determine the significant effect of DS entrapment efficiency, water uptake, swelling and release parameter of the DCA beads. Difference was considered to be significant at a level of $P < 0.05$.

Acknowledgements: The author wishes to thank P. Sri-udon and S. Kanjanabat for laboratory assistance and Faculty of Pharmaceutical Sciences, Khon Kaen University, Khon Kaen, Thailand for technical supports.

References

Almeida PF, Almeida AJ (2004) Cross-linked alginate-gelatin beads: a new matrix for controlled release of pindolol. J Control Release 97: 431–439.

Chebli C, Cartilier L (1998) Cross-linked cellulose as a tablet excipient: A binding/disintegrating agent. Int J Pharm 171: 101–110.

Costa P, Lobo JMS (2001) Modeling and comparison of dissolution profiles. Eur J Pharm Sci 13: 123–133.

Dashevsky A (1998) Protein loss by the microencapsulation of an enzyme (lactase) in alginate beads. Int J Pharm 161: 1–5.

Draget KI (2000) Alginates. In: Philips GO, Williams PA (eds.) Handbook of hydrocolloids, Cambridge, p. 379–395.

Fernández-Hervás MJ, Holgado MA, Fini A, Fell JT (1998) In vitro evaluation of alginate beads of a diclofenac salt. Int J Pharm 163: 23–34.

Grant GT, Morris ER, Rees DA, Smith PJC, Thom D (1973) Biological interaction between polysaccharides and divalent cations: The egg-box model. FEBS Lett 32: 195–198.

Hwang SJ, Rhee GJ, Lee KM, Oh KH, Kim CK (1995) Release characteristics of ibuprofen from excipient-loaded alginate gel beads. Int J Pharm 116: 125–128.

Johansson B, Alderborn G (1996) Degree of pellet deformation during compaction and its relationship the tensile strength of tablets formed of microcrystalline cellulose pellets. Int J Pharm 132: 207–220.

Johansson B, Alderborn G (2001) The effect of shape and porosity on the compression behaviour and tablet forming ability of granular materials formed from microcrystalline cellulose. Eur J Pharm Biopharm 52: 347–357.

Johansson B, Wikberg M, Ek R, Alderborn G (1995) Compression behaviour and compactability of microcrystalline cellulose pellets in relationship to their pore structure and mechanical properties. Int J Pharm 117: 57–73.

Kikuchi A, Kawabuchi M, Sugihara M, Sakurai Y, Okano T (1997) Pulsed dextran release from calcium-alginate gel beads. J Control Release 47: 21–29.

Kim MS, Park GD, Jun SW, Lee S, Park JS, Hwang SJ (2005) Controlled release tamsulosin hydrochloride from alginate beads with waxy materials. J Pharm Pharmacol 57: 1521–1528.

Lee PI, Peppas NA (1987) Prediction of polymer dissolution in swellable controlled-release systems. J Control Release 6: 207–215.

Murata Y, Miyamoto E, Kawashima S (1996) Additive effect of chondroitin sulfate and chitosan on drug release from calcium-induced alginate gel beads. J Control Release 38: 110–108.

Murata Y, Nakada K, Miyamoto E, Kawashima S, Seo SH (1993) Influence of erosion of calcium-induced alginate gel matrix on the release of Brilliant Blue. J Control Release 23: 21–26.

Murata Y, Tsumoto K, Kofuji K, Kawashima S (2002) Effect of natural polysaccharide addition on drug release from calcium-induced alginate gel beads. Chem Pharm Bull 51: 218–220.

Østberg T, Lund EM, Graffner C (1994) Calcium alginate matrices for oral multiple unit administration: IV release characteristics in different media. Int J Pharm 112: 241–248.

Palomo ME, Ballesteros MP, Frutos P (1999) Analysis of diclofenac sodium and derivatives. J Pharm Biomed Anal 21: 83–94.

Pongjanyakul T, Puttipipatkhachorn S (2007) Xanthan-alginate composite gel beads: molecular interaction and in vitro characterization. Int J Pharm 331: 61–71.

Pongjanyakul T, Sungtongjeen S, Puttipipatkhachorn S (2006) Modulation of drug release from glyceryl palmitostearate-alginate beads via heat treatment. Int J Pharm 319: 20–28.

Puttipipatkhachorn S, Pongjanyakul T, Priprem A (2005) Molecular interaction in alginate beads reinforced with sodium starch glycolate or magnesium aluminum silicate, and their physical characteristics. Int J Pharm 293: 51–62.

Remuñán-López C, Bodmeier R (1997) Mechanical, water uptake and permeability properties of crosslinked chitosan glutamate and alginate films. J Control Release 44: 215–225.

Sheu MT, Chou HL, Kao CC, Liu CH, Sokoloski TD (1992) Dissolution of diclofenac sodium from matrix tablets. Int J Pharm 85: 57–63.

Sugawara S, Imai T, Otagiri M (1994) The controlled release of prednisolone using alginate gel. Pharm Res 11: 272–277.

Talukdar MM, Kinget R (1995) Swelling and drug release behaviour of xanthan gum tablets. Int J Pharm 120: 63–72.

Tudja P, Khan MZI, Meštrović E, Horvat M, Golja P (2001) Thermal behaviour of diclofenac sodium: decomposition and melting characteristics. Chem Pharm Bull 49: 1245–1250.

Wade A, Weller PJ (1994) Handbook of pharmaceutical excipients, 2nd ed., Washington and London, p. 84–87.

Wang K, He Z (2002) Alginate-konjac glucomannan-chitosan beads as controlled release matrix. Int J Pharm 244: 117–126.